

Pair production of neutral Higgs bosons from the left-right twin Higgs model via $\gamma\gamma$ collisions^{*}

MA Wei(马威) YUE Chong-Xing(岳崇兴)¹⁾ ZHANG Ting-Ting(张婷婷)

Department of Physics, Liaoning Normal University, Dalian 116029, China

Abstract: The left-right twin Higgs (LRTH) model predicts the existence of the neutral Higgs bosons (h, ϕ^0), which can be produced in pairs ($\phi^0\phi^0, hh, \phi^0h$) via $\gamma\gamma$ collisions at the next generation e^+e^- International Linear Collider (ILC). Our numerical results show that the production cross section of the neutral Higgs boson pair $\phi^0\phi^0$ can reach 8.8 fb. The subprocess $\gamma\gamma \rightarrow \phi^0\phi^0$ might be used to test the LRTH model in future ILC experiments.

Key words: neutral Higgs bosons, left-right twin Higgs model, $\gamma\gamma$ collisions

PACS: 14.80.Ec, 12.60.Fr, 12.15.Ji **DOI:** 10.1088/1674-1137/35/4/003

1 Introduction

To solve the fine tuning problem of the SM, many new physics models have been proposed. However, a so-called “little hierarchy problem” [1] arises in these models, once constraints from precision measurements are imposed. Many alternative new physics models with extended Higgs sectors, for instance the little Higgs models [2] and the left-right twin Higgs (LRTH) model [3], can solve the above difficulty, which predict the existence of the neutral Higgs bosons.

The hunt for Higgs bosons is one of the most important goals of the Large Hadron Collider (LHC). If a Higgs boson is discovered at the LHC, it will be crucial to determine its couplings with high accuracy. The high resolution profile determination of a Higgs boson (mass, couplings, self-couplings, etc.) can be carried out at the next generation e^+e^- International Linear Collider (ILC) [4]. Physics at the LHC and at the ILC will be complementary to each other in many respects [5]. In such a collider, in addition to e^+e^- collision, one can also realize $\gamma\gamma$ collision with the photon beams generated by the backward Compton scattering of incident electron and laser beams. The $\gamma\gamma$ collision offers a unique opportunity to explore new physics effects through production mecha-

nisms that are not accessible in leptonic or hadronic machines [6].

Pair production of the Higgs bosons via $\gamma\gamma$ collisions at the ILC will provide a way to test the Higgs boson self-coupling, which may be sensitive to new physics [7]. So far, there has been much work to study pair production of the Higgs bosons via $\gamma\gamma$ collisions in the SM [8], in some popular physics models beyond the SM [9], and model independently [10]. The LRTH model [3] predicts the existence of one SM-like neutral Higgs h and one neutral pseudoscalar Higgs ϕ^0 . The neutral Higgs boson pairs can be produced via the subprocesses $\gamma\gamma \rightarrow \phi^0\phi^0, \gamma\gamma \rightarrow hh$ and $\gamma\gamma \rightarrow \phi^0h$ at the ILC. The main aim of this paper is to study pair production of the neutral Higgs bosons predicted by the left-right twin Higgs (LRTH) model [3] via these processes at the ILC, and see whether the possible signatures of the LRTH model can be detected via these production processes in future ILC experiments.

This paper is organized as follows. In Sec. 2, we briefly review the essential features of the LRTH model. The effective production cross sections of the subprocesses $\gamma\gamma \rightarrow \phi^0\phi^0, \gamma\gamma \rightarrow hh$ and $\gamma\gamma \rightarrow \phi^0h$ are calculated in Sec. 3. The relevant phenomenological analyses are also given in Sec. 3. Our conclusions are given in Sec. 4.

Received 16 July 2010, Revised 15 August 2010

^{*} Supported by National Natural Science Foundation of China (10975067), Specialized Research Fund for the Doctoral Program of Higher Education (SRFDP) (200801650002), Natural Science Foundation of Liaoning Scientific Committee (20082148) and Foundation of Liaoning Educational Committee (2007T086)

1) E-mail: cxyue@lnnu.edu.cn

©2011 Chinese Physical Society and the Institute of High Energy Physics of the Chinese Academy of Sciences and the Institute of Modern Physics of the Chinese Academy of Sciences and IOP Publishing Ltd

2 The left-right twin Higgs model

Recently, the twin Higgs mechanism [11] has been proposed as a solution to the little hierarchy problem. The twin Higgs mechanism can be implemented in left-right models with the additional discrete symmetry being identified with left-right symmetry [3]. The details of the model as well as the particle spectrum, Feynman rules, and some phenomenology analysis have been studied in Refs. [12, 13]. Here we will briefly review the essential features of the model and focus our attention on the neutral Higgs bosons.

The LRTH model [3] is based on the global $U(4)_1 \times U(4)_2$ symmetry with a locally gauged subgroup $SU(2)_L \times SU(2)_R \times U(1)_{B-L}$. Two Higgs fields, $H = (H_L, H_R)$ and $\hat{H} = (\hat{H}_L, \hat{H}_R)$, are introduced and each transforms as $(4, 1)$ and $(1, 4)$, respectively, under the global symmetry. $H_{L,R}$ ($\hat{H}_{L,R}$) are two components which are charged under $SU(2)_L$ and $SU(2)_R$, respectively. After the re-parametrization of the fields, there are one neutral pseudoscalar ϕ^0 , a pair of charged scalar ϕ^\pm , the SM-like Higgs boson h , and a $SU(2)_L$ doublet $\hat{h} = (\hat{h}_1^+, \hat{h}_2^0)$.

The $U(4)_1 [U(4)_2]$ group is spontaneously broken down to its subgroup $U(3)_1 [U(3)_2]$ with nonzero vacuum expectation value (VEV) $\langle H \rangle = (0, 0, 0, f)$ [$\langle \hat{H} \rangle = (0, 0, 0, \hat{f})$]. The Higgs VEVs also break $SU(2)_R \times U(1)_{B-L}$ down to the SM $U(1)_Y$. After spontaneous global symmetry breaking, three Goldstone bosons are eaten by the new gauge bosons W_H^\pm and Z_H . After the SM electroweak symmetry breaking, the three additional Goldstone bosons are eaten by the SM gauge bosons W^\pm and Z .

The Higgs bosons h and ϕ^0 can couple to each other, and can also couple to ordinary fermions, ordinary gauge bosons, the new top quark T , and the new gauge bosons Z_H and W_H . The coupling expressions, which are related to our calculations, are shown as [12]

$$\begin{aligned} & hhW_\mu^+ W_\nu^- : e^2 g_{\mu\nu} / (2s_W^2), h\bar{t}t : -em_t C_L C_R / (2m_W s_W), \\ & A_\mu \bar{T}T : 2e\gamma_\mu / 3; hhW_{H\mu}^+ W_{H\nu}^- : -e^2 g_{\mu\nu} / (2s_W^2), \\ & h\bar{T}T : -y(S_R S_L - C_L C_R x) / \sqrt{2}, hW_\mu^+ W_\nu^- : \\ & em_W g_{\mu\nu} / s_W; \phi^0 \phi^0 W_\mu^+ W_\nu^- : -e^2 g_{\mu\nu} / (54s_W^2), \\ & \phi^0 \bar{t}t : -iyS_R S_L \gamma_5 / \sqrt{2}, hW_{H\mu}^+ W_{H\nu}^- : -e^2 f x g_{\mu\nu} / (2s_W^2); \\ & \phi^0 \phi^0 W_{H\mu}^+ W_{H\nu}^- : e^2 g_{\mu\nu} / (2s_W^2), \phi^0 \bar{T}T : \\ & -iyC_L C_R \gamma_5 / \sqrt{2}, h\phi^0 \phi^0 : \\ & x(30p_2 \cdot p_3 + 11p_1 \cdot p_1) / (27\sqrt{2}f), \end{aligned}$$

where p_1, p_2 , and p_3 refer to the incoming momentums of the first, second, and third particles, respectively. $x = v/\sqrt{2}f$, $s_W = \sin\theta_W$, and θ_W is the Weinberg angle. At the leading order of $1/f$, the sine values of the mixing angles α_L and α_R can be written as $S_L = \sin\alpha_L \approx \frac{M}{M_T} \sin x$ and $S_R = \sin\alpha_R \approx \frac{M}{M_T} (1 + \sin^2 x)$, with $C_L^2 = 1 - S_L^2$ and $C_R^2 = 1 - S_R^2$. In the following section, we will use the above Feynman rules to calculate the effective production cross sections of the subprocesses $\gamma\gamma \rightarrow \phi^0 \phi^0$, $\gamma\gamma \rightarrow hh$ and $\gamma\gamma \rightarrow \phi^0 h$ at the ILC.

3 Production of the neutral Higgs boson pairs

3.1 $\phi^0 \phi^0$ production

The subprocess $\gamma\gamma \rightarrow \phi^0 \phi^0$ is loop-induced at the lowest order, as shown in Fig. 1. The Feynman diagrams created by exchanging the initial photons or the final Higgs bosons, which are not shown in Fig. 1, are also involved in our calculations. The one-loop calculation can be carried out by summing all unrenormalized reducible and irreducible one-loop diagrams and the results will be finite and gauge invariant. Each loop diagram is composed of some scalar loop functions, which are calculated by using Loop Tools [14].

The expression of the amplitude for the subprocess $\gamma(k_1) + \gamma(k_2) \rightarrow \phi^0(p_1) + \phi^0(p_2)$ can be written as $\mathcal{M} = \mathcal{M}_a + \mathcal{M}_b + \mathcal{M}_c + \mathcal{M}_d$ with

$$\begin{aligned} \mathcal{M}_a^{(i)} &= a^i \epsilon_\mu(k_1) \epsilon_\nu(k_2) \left\{ \frac{2}{3} C_\rho C_\sigma \epsilon^{\rho\mu\sigma\nu} - C_\rho \epsilon^{\rho\mu\sigma\nu} k_{1\sigma} \right. \\ &\quad \left. + \frac{1}{3} C_0 \epsilon^{\rho\nu\sigma\mu} k_{1\rho} k_{2\sigma} + \frac{1}{3} C_\rho \epsilon^{\rho\sigma\mu\nu} k_{1\sigma} - \frac{1}{3} k_1^2 C_0 g^{\mu\nu} \right. \\ &\quad \left. - \frac{1}{3} C_0 \epsilon^{\rho\sigma\mu\nu} k_{1\rho} k_{2\sigma} \right\}, \\ \mathcal{M}_c^{(j)} &= c^j \epsilon_\mu(k_1) \epsilon_\nu(k_2) \{ 5C_\rho C_\sigma \epsilon^{\rho\mu\sigma\nu} - 5C_\rho \epsilon^{\rho\mu\sigma\nu} k_{1\sigma} \\ &\quad + 2C_\rho \epsilon^{\rho\sigma\mu\nu} k_{1\sigma} - C_0 \epsilon^{\rho\sigma\mu\nu} k_{1\rho} k_{2\sigma} \\ &\quad - 6C_0 \epsilon^{\rho\nu\sigma\mu} k_{1\rho} k_{2\sigma} + 3C_\rho \epsilon^{\rho\sigma\mu\nu} k_{2\sigma} \}, \end{aligned}$$

where $i = 1$ for top-loop, $i = 2$ for heavy top-loop, $j = 1$ for W-loop, $j = 2$ for W_H -loop, a^i and c^j are the coefficients¹⁾ of the corresponding amplitudes, C_0 and $C_{\rho(\sigma)}$ are three-point standard functions²⁾.

1) These constants can be found in Appendix A.

2) The expression forms of these three-point standard functions can be found in Appendix A.

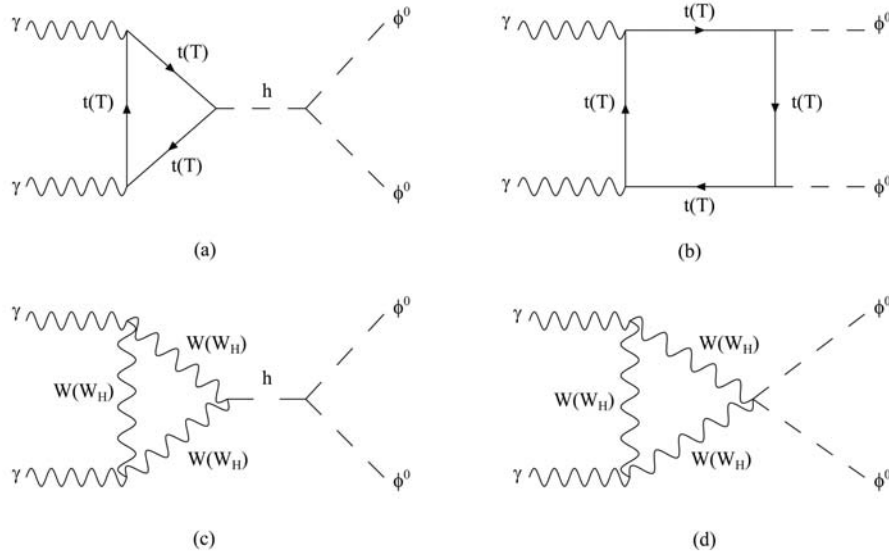


Fig. 1. One-loop Feynman diagrams for the subprocess $\gamma\gamma \rightarrow \phi^0\phi^0$ in the LRTH model. The diagrams obtained by exchanging the two photons or exchanging the two Higgs bosons are not shown here.

Because the expression form of \mathcal{M}_b is lengthy, and \mathcal{M}_d is very similar to \mathcal{M}_c except for the relevant coefficients, we do not present them here. But our numerical results have summed all of their contributions.

From the above discussions, we can see that, except for the SM input parameters $\alpha = 1/128.8$, $s_W = \sqrt{0.2315}$, $m_W = 80.574$ GeV [15], the production cross sections of the Higgs boson pairs $\phi^0\phi^0$, hh and ϕ^0h at the ILC are dependent on the model dependent parameters f , M and the masses of the Higgs boson ϕ^0 . In this paper, we will fix $M = 150$ GeV. The value of f is bounded from electroweak precision measurements, which cannot be too large since the fine tuning is more severe for larger f . In the LRTH model, the mass of the neutral Higgs boson ϕ^0 is a free parameter, but is usually taken to be about 100 GeV [3]. In this paper, we consider that it is in the range of $120 \text{ GeV} \leq m_{\phi^0} \leq 180$ GeV. In Fig. 2, we plot the effective cross section σ of the subprocess $\gamma\gamma \rightarrow \phi^0\phi^0$ as a function of the scale parameter f for the c.m. energy $\sqrt{s} = 500$ GeV and three values of the ϕ^0 mass m_{ϕ^0} . We can see that σ is sensitive to the scale parameter f , while it is not sensitive to the mass parameter m_{ϕ^0} . Its value decreases as the scale parameter f increases. For $500 \text{ GeV} \leq f \leq 1500$ GeV and $120 \text{ GeV} \leq m_{\phi^0} \leq 180$ GeV, its value is in the range of 0.04–2.28 fb. If we assume the integrated luminosity $\mathcal{L}_{\text{int}} = 100 \text{ fb}^{-1}$ for the ILC with the c.m. energy $\sqrt{s} = 500$ GeV, there will be 4–228 $\phi^0\phi^0$ events to be generated.

In order to see the effects of the c.m. energy \sqrt{s} on the effective cross section σ , we plot σ as a function

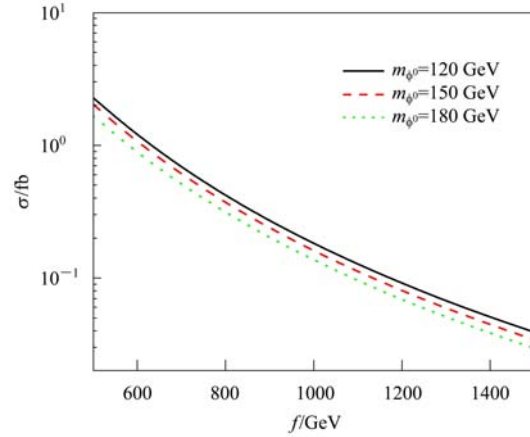


Fig. 2. The effective cross section σ of the subprocess $\gamma\gamma \rightarrow \phi^0\phi^0$ as a function of f for $\sqrt{s} = 500$ GeV and three values of m_{ϕ^0} .

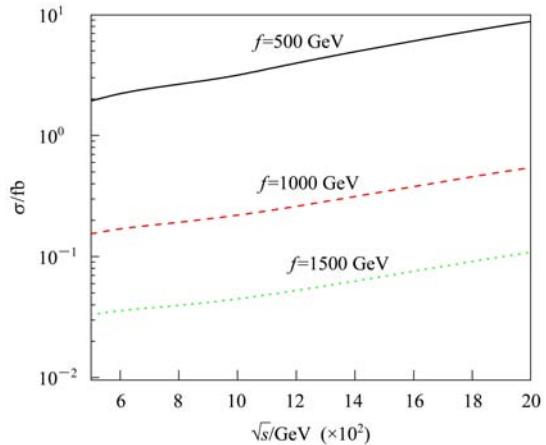


Fig. 3. The effective cross section σ of the subprocess $\gamma\gamma \rightarrow \phi^0\phi^0$ as a function of \sqrt{s} for $m_{\phi^0} = 150$ GeV and three values of f .

of \sqrt{s} for three values of the scale parameter f in Fig. 3. We can see that, for $f=1$ TeV, $500 \text{ GeV} \leq \sqrt{s} \leq 2000 \text{ GeV}$ and $m_{\phi^0}=150 \text{ GeV}$, the value of σ is in the range of 0.15–0.54 fb.

3.2 hh production

The Feynman diagrams of the subprocess $\gamma\gamma \rightarrow hh$ are shown in Fig. 4. In our numerical calculation, we also consider the Feynman diagrams created by initial photons exchanged or the final Higgs bosons exchanged. The amplitudes of Fig. 4(a) and Fig. 4(b) are quite similar to Fig. 1(d) and Fig. 1(b), respectively. To save space, we do not show them here.

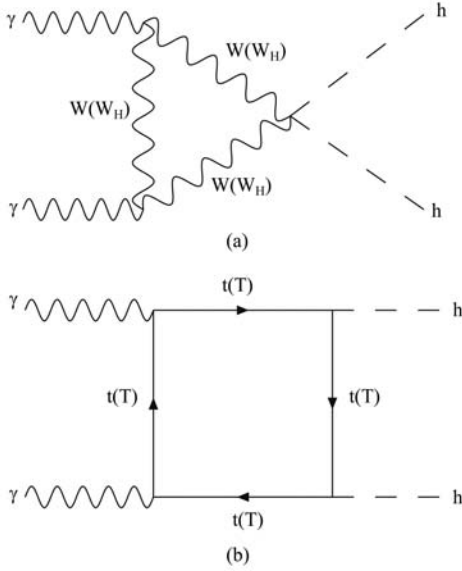


Fig. 4. Feynman diagrams for the subprocess $\gamma\gamma \rightarrow \phi^0 h$ in the LRTH model.

We plot the effective cross section σ of the subprocess $\gamma\gamma \rightarrow hh$ as a function of the c.m. energy \sqrt{s} for $f=500 \text{ GeV}$ and three values of m_h in Fig. 5. It is obvious that, in most of the parameter space, the effective cross section σ is smaller than that of the subprocess $\gamma\gamma \rightarrow \phi^0 \phi^0$, which is because the cross section of the subprocess $\gamma\gamma \rightarrow \phi^0 \phi^0$ mainly comes from the contributions of Fig. 1(a), while the Feynman diagrams of the subprocess $\gamma\gamma \rightarrow hh$ do not include the similar Feynman diagrams. For $f=500 \text{ GeV}$ and $\sqrt{s}=2000 \text{ GeV}$, the value of σ can reach 0.21 fb. If we assume the integrated luminosity $\mathcal{L}_{\text{int}} = 100 \text{ fb}^{-1}$, there will be only several hh events to be generated, and it is very difficult to detect the possible signals of the neutral Higgs boson h via the subprocess $\gamma\gamma \rightarrow hh$ in future ILC experiments.

3.3 $\phi^0 h$ production

The Feynman diagrams of the subprocess $\gamma\gamma \rightarrow \phi^0 h$ are shown in Fig. 6. The expression form of the

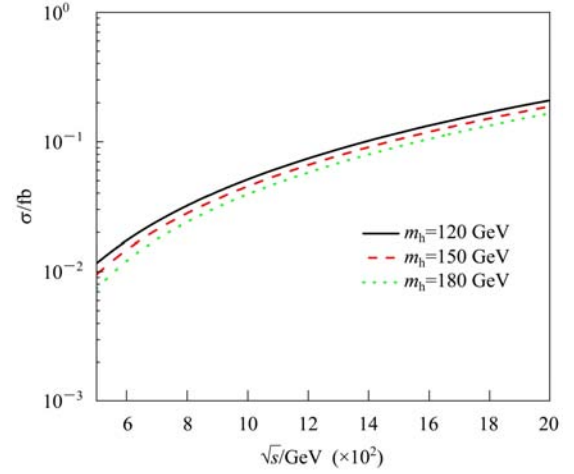


Fig. 5. The effective cross section σ of the subprocess $\gamma\gamma \rightarrow hh$ as a function of \sqrt{s} for $f=500 \text{ GeV}$ and three values of m_h .

amplitude for the subprocess $\gamma(k_1) + \gamma(k_2) \rightarrow \phi^0(p_1) + h(p_2)$ can be written as $\mathcal{M} = \mathcal{M}_a + \mathcal{M}_b$ with

$$\begin{aligned} \mathcal{M}_a^{\text{t-loop}} &= \frac{ye^2 S_L S_R x (30p_1 p_2 + p_{12}^2) m_t}{243\sqrt{2} f p_{12}^2 \pi^2} \\ &\quad \times C_0 \epsilon_\mu(k_1) \epsilon_\nu(k_2) \epsilon^{k_1 k_2 \mu \nu}, \\ \mathcal{M}_a^{\text{T-loop}} &= \frac{ye^2 C_L C_R x (30p_1 p_2 + p_{12}^2) m_T}{243\sqrt{2} f p_{12}^2 \pi^2} \\ &\quad \times C_0 \epsilon_\mu(k_1) \epsilon_\nu(k_2) \epsilon^{k_1 k_2 \mu \nu}. \end{aligned}$$

Where $p_{12} = p_1 + p_2$, the three-point standard functions $C_{0(t)} = C_0(k_1, k_2, m_t, m_t, m_t)$, $C_{0(T)} = C_0(k_1, k_2, m_T, m_T, m_T)$. Because the expression of \mathcal{M}_b is too lengthy, we do not present it here.

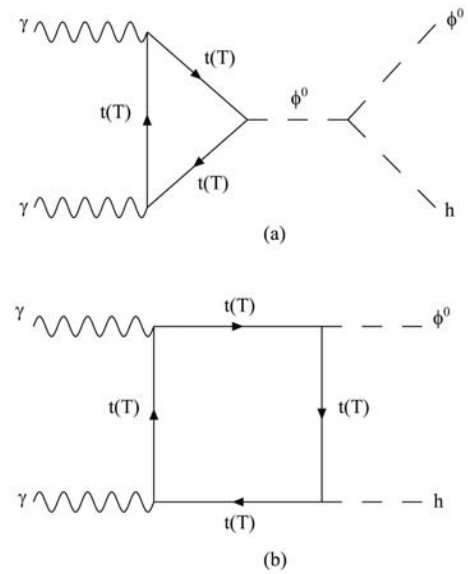


Fig. 6. One-loop Feynman diagrams for the subprocess $\gamma\gamma \rightarrow \phi^0 h$ in the LRTH model.

In Fig. 7, we plot the effective cross section σ of the subprocess $\gamma\gamma \rightarrow \phi^0 h$ as a function of the scale parameter f for the c.m. energy $\sqrt{s}=500$ GeV and three values of m_{ϕ^0} . In our numerical estimation, we have assumed that the mass of the neutral Higgs boson ϕ^0 is equal to that of the neutral Higgs boson h . For $120 \text{ GeV} \leq m_{\phi^0} \leq 180 \text{ GeV}$, $500 \text{ GeV} \leq f \leq 1500 \text{ GeV}$ and $\sqrt{s}=500$ GeV, its values are in the range of $6 \times 10^{-4} \text{ fb} - 9.7 \times 10^{-2} \text{ fb}$. So we can conclude that it is impossible to detect the possible signals of the neutral Higgs boson ϕ^0 via the subprocess $\gamma\gamma \rightarrow \phi^0 h$ in future ILC experiments.

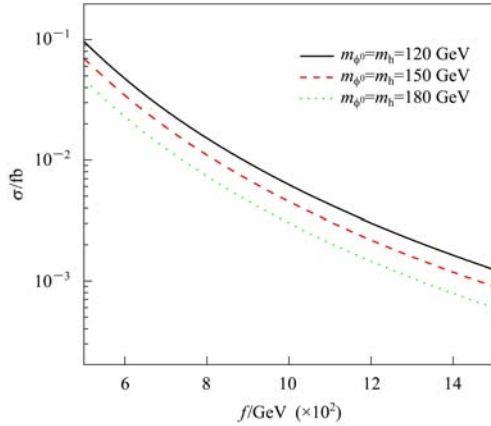


Fig. 7. The effective cross section σ of the subprocess $\gamma\gamma \rightarrow \phi^0 h$ as a function of f for $\sqrt{s}=500$ GeV and three values of m_{ϕ^0} .

The neutral Higgs boson ϕ^0 predicted by the LRTH model mainly decays to $b\bar{b}$. When we analyze the signatures of the neutral Higgs boson pairs at the ILC, we will take the $\phi^0\phi^0$ pair as an example. If we assume that both of these two neutral Higgs bosons decay to $b\bar{b}$, then pair production of the neutral Higgs boson $\phi^0\phi^0$ can give rise to the $b\bar{b}b\bar{b}$ final state, and the production rate of the $b\bar{b}b\bar{b}$ final state can be easily estimated using the formula $\sigma_s \approx \sigma \times Br(\phi^0 \rightarrow b\bar{b}) \times Br(\phi^0 \rightarrow b\bar{b})$. In Fig. 8, we plot the number of $b\bar{b}b\bar{b}$ events as a function of the scale parameter f for the c.m. energy $\sqrt{s}=500$ GeV, $\mathcal{L}_{\text{int}} = 100 \text{ fb}^{-1}$ and three values of m_{ϕ^0} . One can see from Fig. 8 that, for $f=500$ GeV, $120 \text{ GeV} \leq m_{\phi^0} \leq 180 \text{ GeV}$, the number of $b\bar{b}b\bar{b}$ events is in the range of 1–70, which is significantly larger than that for the SM Higgs boson pair production process $\gamma\gamma \rightarrow hh \rightarrow b\bar{b}b\bar{b}$ [16].

The dominant backgrounds of the $b\bar{b}b\bar{b}$ signals come from the process $\gamma\gamma \rightarrow W^+W^-$ with the gauge boson W decaying to quarks and non-resonant four jet production. Detailed analyses of the signals and the relevant backgrounds have been given in Ref. [17]. They have shown that the first one can be reduced

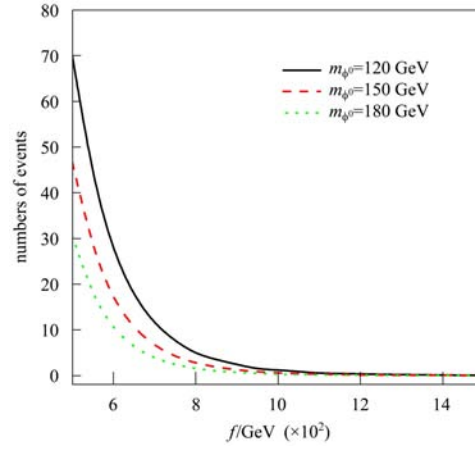


Fig. 8. The number of the $b\bar{b}b\bar{b}$ events as a function of f for $\sqrt{s}=500$ GeV, $\mathcal{L}_{\text{int}} = 100 \text{ fb}^{-1}$ and three values of m_{ϕ^0} .

by imposing an appropriate cut on the invariant mass $m(b\bar{b})$ of each pair of b -jets, forcing it to be close to the Higgs mass. The second one, non-resonant four jet background, can be eliminated by imposing a cut on the polar angle. Therefore, we hope that by imposing appropriate cuts on the invariant mass and the polar angle and using efficient b -tagging, it is possible to detect the signatures of the neutral Higgs boson ϕ^0 via the subprocess $\gamma\gamma \rightarrow \phi^0\phi^0 \rightarrow b\bar{b}b\bar{b}$ in future ILC experiments.

4 Conclusions

The LRTH model predicts the existence of neutral scalar particles. If possible, signals of these new particles can be detected in future experiments, which will be important for testing the LRTH model and the EWSB mechanism. In this paper, we consider the pair production of neutral Higgs bosons predicted by the LRTH model via $\gamma\gamma$ collisions, and discuss their possible signatures in future ILC experiments.

We calculate the effective production cross sections of the neutral Higgs boson pairs via the subprocesses $\gamma\gamma \rightarrow \phi^0\phi^0$, $\gamma\gamma \rightarrow hh$ and $\gamma\gamma \rightarrow \phi^0 h$ at the ILC. Our numerical results show that the production rates of the neutral Higgs boson pairs mainly depend on the scale parameter f and the c.m. energy \sqrt{s} . In most of the parameter space, the effective cross section σ of the subprocesses $\gamma\gamma \rightarrow \phi^0\phi^0$ is larger than that for the second or third subprocesses. For $500 \text{ GeV} \leq f \leq 1500 \text{ GeV}$, $500 \text{ GeV} \leq \sqrt{s} \leq 2000 \text{ GeV}$ and $120 \text{ GeV} \leq m_{\phi^0} \leq 180 \text{ GeV}$, $\sigma(\gamma\gamma \rightarrow \phi^0\phi^0)$ is in the range of 0.04–8.79 fb, while the value of $\sigma(\gamma\gamma \rightarrow \phi^0 h)$ or $\sigma(\gamma\gamma \rightarrow hh)$ is smaller than 1 fb. Since the neutral Higgs boson ϕ^0 mainly decays to

$\bar{b}b$, its pair production can easily transfer to the $\bar{b}bbb$ final state. If we assume the integrated luminosity $\mathcal{L}_{\text{int}} = 100 \text{ fb}^{-1}$ for the ILC with the c.m. energy $\sqrt{s} = 500 \text{ GeV}$, there will be several and up to sev-

eral hundreds of $\bar{b}bbb$ events to be generated. Thus, the possible signals of the LRTH model might be detected via the subprocess $\gamma\gamma \rightarrow \phi^0\phi^0$ in future ILC experiments.

Appendix A

In this appendix, we give the relevant coefficients and the three-point standard functions related to our calculations.

The coefficients for the amplitude of Fig. 1(a) are given by

$$a^{\text{t-loop}} = \frac{ie^3 m_t^2 C_L C_R x (30p_1 p_2 + 11p_{12}^2)}{162\sqrt{2} f m_W s_W p_{12}^2 \pi^2};$$

$$a^{\text{T-loop}} = \frac{ie^3 m_T^2 C_L C_R x (30p_1 p_2 + 11p_{12}^2)}{162\sqrt{2} f m_W s_W p_{12}^2 \pi^2},$$

where $p_{12} = p_1 + p_2$.

The three-point standard functions C_0 and C_ρ in the amplitude of Fig. 1(a) are defined as [18]

$$C_{0(t)} = C_0(k_1, k_2, m_t, m_t, m_t),$$

$$C_{0(T)} = C_0(k_1, k_2, m_T, m_T, m_T),$$

$$C_{11(t)} = C_{11}(k_1, k_2, m_t, m_t, m_t),$$

$$C_{11(T)} = C_{11}(k_1, k_2, m_T, m_T, m_T),$$

$$C_{12(t)} = C_{12}(k_1, k_2, m_t, m_t, m_t),$$

$$C_{12(T)} = C_{12}(k_1, k_2, m_T, m_T, m_T),$$

$$C_{\rho(t)} = k_{1\rho} C_{11(t)} + k_{2\rho} C_{12(t)},$$

$$C_{\rho(T)} = k_{1\rho} C_{11(T)} + k_{2\rho} C_{12(T)}.$$

The coefficients of the amplitude of Fig. 1(c) are given by

$$c^{\text{W-loop}} = \frac{ie^3 m_W x (30p_1 p_2 + 11p_{12}^2)}{432\sqrt{2} f s_W p_{12}^2 \pi^2};$$

$$c^{\text{W}_H\text{-loop}} = \frac{ie^4 x^2 (30p_1 p_2 + 11p_{12}^2)}{864\sqrt{2} s_W^2 p_{12}^2 \pi^2}.$$

The three-point standard functions C_0 and C_ρ in the amplitude of Fig. 1(c) are defined as

$$C_{0(W)} = C_0(k_1, k_2, m_W, m_W, m_W),$$

$$C_{0(W_H)} = C_0(k_1, k_2, m_{W_H}, m_{W_H}, m_{W_H}),$$

$$C_{11(W)} = C_{11}(k_1, k_2, m_W, m_W, m_W),$$

$$C_{11(W_H)} = C_{11}(k_1, k_2, m_{W_H}, m_{W_H}, m_{W_H}),$$

$$C_{12(W)} = C_{12}(k_1, k_2, m_W, m_W, m_W),$$

$$C_{12(W_H)} = C_{12}(k_1, k_2, m_{W_H}, m_{W_H}, m_{W_H}),$$

$$C_{\rho(W)} = k_{1\rho} C_{11(W)} + k_{2\rho} C_{12(W)},$$

$$C_{\rho(W_H)} = k_{1\rho} C_{11(W_H)} + k_{2\rho} C_{12(W_H)}.$$

References

- Barbieri R, Strumia A. Phys. Lett. B, 1999, **462**: 144
- Schmaltz M, Tucker-Smith D. Ann. Rev. Nucl. Part. Sci., 2005, **55**: 229; Perelstein M. Prog. Part. Nucl. Phys., 2007, **58**: 247
- Chacko Z, Goh H S, Harnik R. JHEP, 2006, **0601**: 108
- Brau J et al. (ILC collaboration). ILC Reference Design Report Volume 1 - Executive Summary, arXiv: 0712.1950 [physics.acc-ph]; Aarons G et al. (ILC collaboration). International Linear Collider Reference Design Report Volume 2: PHYSICS AT THE ILC, arXiv: 0709.1893 [hep-ph]
- Weiglein G et al. (ILC/LC Study Group). Phys. Rept., 2006, **426**: 47
- Ginzburg I F. arXiv: 0912.4841 [hep-ph]
- Baur U et al. Phys. Rev. Lett., 2002, **89**: 151801; Moretti M et al. JHEP, 2005, **0502**: 024; Binoth T et al. Phys. Rev. D, 2006, **74**: 113008
- Jikia G V. Nucl. Phys. B, 1994, **412**: 57; Belusevic R, Jikia G. Phys. Rev. D, 2004, **70**: 073017
- Moretti S et al. Eur. Phys. J. C, 2003, **29**: 19; Wang L et al. Phys. Rev. D, 2005, **72**: 095005; Arhrib A, Benbrik R, Chen C H, Santos R. Phys. Rev. D, 2009, **80**: 015010; ZHU S H, LI C S, GAO C S. Phys. Rev. D, 1998, **58**: 015006; Gounaris G J et al. Eur. Phys. J. C, **18**: 181; JIN Z Y et al. Phys. Rev. D, 2003, **68**: 093004; Cornet F, Hollik W. Phys. Lett. B, 2008, **669**: 58; Asakawa E et al. Phys. Lett. B, 2009, **672**: 354; HE X G. Phys., Rev. D, 1999, **60**: 115017; CHEN C Y. arXiv: 0809.0100; Atwood D, Bar-Shalom S, Soni A. Phys. Rev. D, 2007, **76**: 033004; Arhrib A, Benbrik R, CHEN C H, Santos R. Phys. Rev. D, 2009, **80**: 015010
- CHAO D B et al. Phys. Lett. B, 1993, **315**: 399; Smith J et al. Nucl. Phys. Proc. Suppl., 2003, **116**: 164
- Barbieri R, Gregoire T, Hall L J. arXiv: 0509242; Goh H S, Krenke C A. Phys. Rev. D, 2007, **76**: 115018; Falkowski A, Pokorski S, Schmaltz M. Phys. Rev. D, 2006, **74**: 035003; Chacko Z, Goh H S, Harnik R. Phys. Rev. Lett., 2006, **96**: 231802
- Goh H S, SU S. Phys. Rev. D, 2007, **75**: 075010
- Abada A, Hidalgo I. Phys. Rev. D, **77**: 113013; Dolle E M, SU S. Phys. Rev. D, 2008, **77**: 075013; YUE C X, YANG H D, MA W. Nucl. Phys. B, 2009, **818**: 1; Goh H S, Krenke C A. arXiv: 0911.5567
- Hahn T, Perez-Victoria M. Computl. Phys. Commun., 1999, **118**: 153; Hahn T. Nucl. Phys. Proc. Suppl., 2004, **135**: 333
- YAO W M et al. (Particle Data Group). J. Phys. G, 2006, **33**: 1
- Brinkmann R et al. Nucl. Instrum. Methods A, 1998, **406**: 13; Ginzburg I F. Nucl. Phys. Proc. Suppl., 2000, **82**: 367; Boos E et al. Nucl. Instrum. Methods A, 2001, **472**: 100
- Telnov V I. Int. J. Mod. Phys. A, 1998, **13**: 2399; Telnov V I. Nucl. Instrum. Methods A, 2000, **455**: 63
- Hoof G. 't, Veltman M. Nucl. Phys. B, 1979, **153**: 365; Passarino G, Veltman M. Nucl. Phys. B, 1979, **160**: 151